Journal of Magnetic Resonance **145,** 1–7 (2000)
doi:10.1006/jmre.2000.2019, available online at http://www.idealibrary.com on IDEAL®

Tunneling Spectroscopy from Magnetization Evolution in a Tilted Rotating Frame of Nuclear Spins

A. Damyanovich,* J. Peternelj,† and M. M. Pintar‡

*Department of Medical Imaging, University of Toronto, Toronto, Ontario, Canada; †Faculty of Civil and Geodetic Engineering, University of Ljubljana, and Institute J. Stefan, Ljubljana, Slovenia; and ‡Department of Physics, University of Waterloo, Waterloo, Ontario, Canada, N2L 3G1

Received December 1, 1998; revised December 22, 1999

The time evolution of the proton Zeeman magnetization in the rotating frame at the magic angle $\Theta_M = \cos^{-1}(1/\sqrt{3})$ is calculated for an isolated tunneling methyl group and its Fourier transform is given. The calculation compares well with the experimental spectra of CH_3CD_2I and methylmalonic acid. It is shown that Fourier transform spectroscopy of the magnetization evolution in a tilted RF frame represents an excellent alternative to the analogous experiment performed at exact resonance, resulting in improved resolution and a much better signal-to-noise ratio.

INTRODUCTION

The rotational motion of symmetric atomic groups such as CH_3 or NH_4 is usually hindered in molecular crystals. At low temperatures and in the presence of strong hindering potentials, the rotational wave functions may be adequately represented as linear superpositions of harmonic oscillator states centered at the minima of the hindering potential. For methyl groups in particular, the eigenfunctions of the rotational Hamiltonian H_R,

$$H_R = -\frac{\hbar^2}{2I}\frac{d^2}{d\gamma^2} + V_3(\gamma), \qquad [1]$$

are constructed in such a manner as to represent the irreducible representations of the symmetry group of the hindering potential $V_3(\gamma)$. (I is the moment of inertia of the methyl group, while γ is the angle describing its rotation about its symmetry axis.) If the potential has a threefold symmetry, $V_3(\gamma) = (\frac{1}{2})V_0(1 - \cos 3\gamma)$, the symmetry group is C_3 (*1*), and the eigenfunctions $\psi_n^{(\nu)}(\gamma)$ of H_R are given as

$$\psi_n^{(\nu)}(\gamma) = \frac{1}{\sqrt{3}}\sum_j \epsilon^{sj} H^{(n)}(\gamma - j2\pi/3), \quad j = 0, \pm 1. \qquad [2]$$

The $H^{(n)}(\gamma - j2\pi/3)$ are harmonic oscillator functions centered at the minima of $V_3(\gamma)$; $n = 0, 1, 2, \ldots$, is the torsional or librational quantum number, $\epsilon = e^{i2\pi/3}$, with $\nu \in A, E_a, E_b$ denoting the irreducible representations of the C_3 symmetry group, corresponding to $s = 0$, 1, and -1, respectively. For a given n the rotational energy levels form a degenerate doublet of E symmetry and a singlet of A symmetry. The energy difference between the ground state of A symmetry and the first excited doubly degenerate state of E symmetry (which vanishes in the limit $V_0 \to \infty$) is called the tunneling splitting of the ground state manifold, denoted by $\hbar\omega_T$. Thus,

$$\begin{aligned}\hbar\omega_T &\equiv E_{0R}^{(E)} - E_{0R}^{(A)} \\ &= \langle\psi_0^{(E_a)}|H_R|\psi_0^{(E_a)}\rangle - \langle\psi_0^{(A)}|H_R|\psi_0^{(A)}\rangle \\ &= -3\langle H^{(0)}(\gamma)|H_R|H^{(0)}(\gamma - 2\pi/3)\rangle. \end{aligned} \qquad [3]$$

To obtain this result the small overlap between harmonic oscillator functions centered at neighboring minima of the potential has been neglected; in other words the eigenfunctions [2] are considered normalized in this approximation. Consequently, using Eq. [1] and the expression for the ground state harmonic oscillator function $H^{(0)}(\gamma)$ (as given in most textbooks on quantum mechanics), it follows that

$$\omega_T \cong \frac{3}{2}\,\omega_c e^{-(\pi^2/9)(I\omega_c/\hbar)}\left(\frac{I\omega_c}{\hbar}\right)\left(\frac{\pi^2}{9} - \frac{4}{9}\right), \qquad [4]$$

where, $\omega_c = (9V_0/2I)^{1/2}$ is the classical librational frequency around the minima of the hindering potential. A more accurate expression for ω_T based on WKB pocket states (instead of harmonic oscillator states) is given in Ref. (*2*), while its temperature dependence is discussed in Ref. (*3*). The magnitude of the tunneling frequency is of interest because it relates to the strength and symmetry of the hindering potential which, in turn, reflects interactions between neighboring atomic groups (*4*).

In what follows we will describe a spectroscopic method to measure the tunneling frequency by monitoring the evolution of the magnetization in a tilted rotating frame of nuclear spins. With this aim, let us consider an ensemble of isolated methyl groups embedded in a crystal lattice, subject to an external DC magnetic field $\vec{H}_0$ along the y-axis of the laboratory fixed

1090-7807/00 $35.00

coordinate frame. We propose an investigation of the time evolution of the proton magnetization under the influence of RF pulses (of short duration compared to the spin–lattice relaxation time) while the spins are in thermal equilibrium with the lattice. The RF pulse sequence for the measurement of the Zeeman magnetization in the rotating frame at exact resonance, $M_x(t)$, is as follows: The first $\pi/2$ pulse rotates the equilibrium magnetization $\vec{M}_0$ through 90° into the plane perpendicular to $\vec{H}_0$, where its phase defines the orientation of the transverse axes in the frame of reference rotating about the direction of $\vec{H}_0$. (By convention the $\pi/2$-pulse RF field is directed along the y-axis). The subsequent RF field pulse of duration t is phase-shifted by 90° with respect to the first pulse and therefore oriented along the x-axis of the rotating frame.

Except for the fact that in a tilted rotating frame the frequency of the RF field pulse ω differs from the proton Zeeman frequency ω_0, the situation is analogous to standard spin-locking. Also, instead of a 90° pulse, a θ° pulse with a tipping angle $\theta = \tan^{-1}(\omega_1/(\omega_0 - \omega))$ must be used. The frequency of the θ° pulse is equal to ω_0 with $\omega_1 = \gamma_p H_1$ where H_1 is the magnitude of the field pulse.

When the system under consideration is described by a density matrix instead of a wavefunction, then the expectation value of any operator is calculated as the trace of a product of the operator and the density matrix defined with respect to a chosen coordinate system. The density matrix σ for spins evolving in a tilted rotating frame is given by the equation of motion

$$i\hbar \frac{\partial \sigma}{\partial t} = [H, \sigma], \qquad [5]$$

where H is the corresponding Hamiltonian (see below). Equation [5] is further bounded by the initial condition $\sigma(t = 0) = \sigma(0)$, where the time $t = 0$ refers to the instant when the RF field pulse is switched on. It has been common practice to assume the existence of spin temperature in the rotating frame in which case $\sigma(0)$ can be written as

$$\sigma(0) \propto e^{-\beta_Z H_Z - \beta_L (H_R + H_D^{00}(\theta))}, \qquad [6]$$

where $\beta = 1/kT$, and the spin or Zeeman temperature T_Z in the rotating frame equals the lattice temperature times H_1/H_0. k is the Boltzmann constant, while $H_D^{00}(\theta)$ is the secular part of the dipolar interaction in the rotating frame (see below). In the present calculation we will not use the initial condition [6], but shall only assume that prior to the application of the θ° pulse, the Zeeman-rotational system is in thermal equilibrium with the lattice. Since in many experiments the magnitude H_1' of the θ° pulse is comparable to H_1, it is clear that the evolution of the spin system during the θ° pulse could be significant and should be taken into account. No such evolution was considered in deriving [6], therefore this condition must be modified in the present calculation.

The expression for the proton magnetization $M_x(t)$ along the x-axis of the laboratory frame always refers to the end of the field pulse. In actual experiments, however, the monitored time window, or "point" on the FID, is delayed by an additional time τ after the end of the field pulse. Thus, in order to consistently compare experimental results with calculated ones, the evolution of the Zeeman-rotational system in the time interval τ—during which the spins evolve in the laboratory frame—should also be considered.

The experimental data on CH_3CD_2I and methylmalonic acid corroborate the theoretical results conclusively.

THE HAMILTONIAN OF THE SYSTEM AND THE EQUATION OF MOTION FOR THE DENSITY MATRIX IN THE TILTED ROTATING FRAME

The Hamiltonian describing the dynamics of an isolated methyl group (on a time scale short compared to the spin–lattice relaxation time) is

$$H = H_Z + H_R + H_D + H_{RF}(t), \qquad [7]$$

where the Zeeman Hamiltonian is

$$H_Z = -\hbar\omega_0 I_Z. \qquad [8]$$

I_Z is the z-component of the total spin of the methyl group protons, and $\omega_0 \equiv \gamma_p H_0$ is their Larmor frequency. H_R is the rotational Hamiltonian [1]. In what follows, we shall assume that the strength of the threefold hindering potential $V_3(\gamma)$ is sufficiently large to limit the tunneling frequency ω_T of the methyl group to the range of the dipolar frequency $\omega_D = \gamma_p^2\hbar/R_0^3$. Assuming the proton magnetogyric factor is $\gamma_p = 2.675 \times 10^4$ s^{-1} G^{-1} and the proton–proton distance $R_0 \approx 1.78$ A, we obtain $\omega_D \approx 134$ kHz or $\omega_D/\gamma_p \approx 5$ G.

The dipole–dipole interaction, written in a form similar to (5), is

$$H_D = \hbar\omega_D \sum_{k=-2}^{2} (-1)^k \sum_{i<j} U_{ij}^{-k} V_{ij}^{k}. \qquad [9]$$

The operators U_{ij}^{-k} are

$$U_{ij}^{-k} = (6\pi/5)^{1/2} Y_2^{-k}(\theta_{ij}, \phi_{ij}). \qquad [10]$$

where the spherical harmonics $Y_2^{-k}(\theta_{ij}, \phi_{ij})$ (polar angles (θ_{ij}, ϕ_{ij}) associated with the proton–proton vector $\vec{R}_{ij}$), are defined in (*5*). The spin operators V_{ij}^k are

$$V_{ij}^0 = -(8/3)^{1/2}\left[I_i^0 I_j^0 - \frac{1}{4}(I_i^+ I_j^- + I_i^- I_j^+)\right], \quad [11a]$$

$$V_{ij}^{\pm 1} = \pm(I_i^0 I_j^{\pm 1} + I_i^{\pm 1} I_j^0), \quad [11b]$$

$$V_{ij}^{\pm 2} = -I_i^{\pm 1} I_j^{\pm 1}, \quad [11c]$$

and we have introduced $I_i^0 \equiv I_{iz}$ and $I_i^{\pm 1} = I_{ix} \pm I_{iy}$.

The radiofrequency field applied to the sample is a rotating transverse magnetic field. The corresponding interaction Hamiltonian is

$$H_{\mathrm{RF}}(t) = -\hbar\omega_1(I_x \cos\omega t - I_y \sin\omega t), \quad [12]$$

where $\omega_1 \equiv \gamma_p H_1$ and $I_x \equiv I_{x1} + I_{x2} + I_{x3}$ (similarly for I_y).

The equation of motion for the density matrix in the rotating frame (assuming the frequency of the RF field $\omega \gg \omega_1$) is (*6*),

$$i\hbar\frac{\partial\rho_r}{\partial t} = [-\hbar(\omega_0 - \omega)I_z - \hbar\omega_1 I_x + \hbar\omega_D \sum_{i<j} U_{ij}^0 V_{ij}^0 + H_R, \rho_r]. \quad [13]$$

It is related to the density matrix ρ in the laboratory frame by a unitary transformation

$$\rho = e^{i\omega t I_z}\rho_r e^{-i\omega t I_z}. \quad [14]$$

The $\theta°$ tilted rotating frame is introduced through the transformation (*6*)

$$\sigma = e^{i\theta I_y}\rho_r e^{-i\theta I_y}, \quad [15]$$

whereupon the resulting equation of motion for σ becomes

$$i\hbar\frac{\partial\sigma}{\partial t} = [H_0 + V, \sigma], \quad [16]$$

where

$$H_0 = -\hbar\omega_e I_z + H_R + H_D^{00}(\theta), \quad [17]$$

$$H_D^{00}(\theta) = d_{00}(\theta)\hbar\omega_D \sum_{i<j} U_{ij}^0 V_{ij}^0, \quad [18]$$

and

$$V = \sum_{k\neq 0} d_{0k}(\theta)\left(\hbar\omega_D \sum_{i<j} U_{ij}^0 V_{ij}^k\right) \equiv \sum_{k\neq 0} d_{0k}(\theta) V^k. \quad [19]$$

The coefficients $d_{0k}(\theta)$ are (*5*),

$$d_{00}(\theta) = (3\cos^2\theta - 1)/2, \quad [20a]$$

$$d_{0\pm 1}(\theta) = \pm(3/2)^{1/2}\sin\theta\cos\theta, \quad [20b]$$

$$d_{0\pm 2}(\theta) = (3/8)^{1/2}\sin^2\theta. \quad [20c]$$

The effective Zeeman frequency in the tilted rotating frame ω_e, introduced in [17], is

$$\omega_e = [(\omega_0 - \omega)^2 + \omega_1^2]^{1/2}. \quad [21]$$

Time Evolution of the Zeeman Polarization in the Tilted Rotating Frame

Equation [16] is formally the same as discussed previously in (*7*) and consequently the same method of solution applies. Using the interaction representation defined by

$$\sigma_I(t) = e^{(i/\hbar)H_0 t}\sigma(t)e^{-(i/\hbar)H_0 t}, \quad [22]$$

one can easily write down the solution for the interaction picture density matrix $\sigma_I(t)$ in a form of perturbation series. Up to the second order in the nonsecular part of the dipolar interaction V, the result is

$$\sigma_I(t) = \sigma_I(0) + \left(-\frac{i}{\hbar}\right)\int_0^t dt_1[V(t_1), \sigma_I(0)] + \left(-\frac{i}{\hbar}\right)^2\int_0^t dt_1\int_0^{t_1} dt_2[V(t_1), [V(t_2), \sigma_I(0)]] + \cdots, \quad [23]$$

where

$$V(t) = e^{(i/\hbar)H_0 t}Ve^{-(i/\hbar)H_0 t}, \quad [24]$$

and, of course, $\sigma_I(0) \equiv \sigma(0)$.

The initial density matrix $\sigma(0)$ describes the state of the system in the tilted rotating frame immediately after the $\theta°$ pulse has been switched off. As already suggested in the Introduction (and previously discussed in (*7*)), the evolution of the spin system during the $\theta°$ pulse should be considered whenever the magnitude of this pulse, H_1', is comparable to the magnitude H_1 of the spin-locking field pulse. This modifies the expression for the initial density matrix $\sigma(0)$ with respect to its usual high-temperature form, [6]. Using the high-temperature approximation (with the $\theta°$ pulse along the negative *y*-axis) and keeping only terms to first order in the dipolar interactions, we obtain

$$\sigma(0) = \sigma_0(0) + \frac{i\beta_L\hbar\omega_0}{Z}\frac{1}{\hbar\omega_1'}\int_0^\theta d\theta' e^{-ih_R(\theta-\theta')} \times \sum_k k d_{0k}(\theta')V^k e^{ih_R(\theta-\theta')} + \cdots, \quad [25]$$

where $\sigma_0(0) \cong (1 + \beta_L \hbar \omega_0 I_z + \cdots)/Z$ is the high-temperature approximation of [6], Z is the partition sum, $h_R \equiv H_R/\hbar\omega_1'$, and $\omega_1' = \gamma_p H_1'$. The second term of [25] thus represents the change in the initial condition for the density matrix, which is due to spin dephasing during the $\theta°$ pulse.

In accordance with what has been said in the Introduction, the Zeeman polarization along the x-axis of the laboratory frame (the x-component of the magnetization) is

$$M_x(t) = \gamma_p \hbar \mathrm{Tr}(\rho(t) I_x). \qquad [26]$$

Using [14] and the inverses of [15] and [22], we can rewrite [26] as

$$\begin{aligned} M_x(t) = {} & \sin\theta \cdot \gamma_p \hbar \mathrm{Tr}\{\sigma_I(t) I_z\} \cos\omega t \\ & + \cos\theta \cdot \gamma_p \hbar \mathrm{Tr}\{\sigma_I(t) e^{(i/\hbar) H_0 t} I_x e^{-(i/\hbar) H_0 t}\} \cos\omega t \\ & + \gamma_p \hbar \mathrm{Tr}\{\sigma_I(t) e^{(i/\hbar) H_0 t} I_y e^{-(i/\hbar) H_0 t}\} \sin\omega t. \end{aligned} \qquad [27]$$

The calculation of the traces in (*27*) is performed in the basis defined by the eigenstates of H_0 (*17*), which in turn are expressed in terms of the symmetry adapted eigenstates of $-\hbar\omega_e I_z + H_R$ (given explicitly in (*7*) together with the diagonalization of H_0). The calculation is particularly simple—although lengthy—in the magic-angle tilted rotating frame corresponding to $\theta = \theta_M = \cos^{-1}(1/\sqrt{3}) \cong 0.3\pi$. In this case $H_D^{00}(\theta_M) \equiv 0$ (since $d_{00}(\theta_M) = 0$), yielding

$$\begin{aligned} M_x(t) = {} & (\sqrt{6}/3) M_0 \cos\omega t - \frac{1}{4}\left(\frac{\omega_D}{\omega_e}\right)^2 (1 - 3\cos^2\beta)^2 \\ & \times \left\{ -\sqrt{2}\sin\omega_e t - \left(\frac{\omega_e}{\omega_1'}\right)\cos\omega_e t \right. \\ & \left. - \sqrt{2}\sin 2\omega_e t + \left(\frac{\omega_e}{\omega_1'}\right)\cos 2\omega_e t \right\} \sin\omega t \\ & + \frac{\sqrt{3}}{16}\left(\frac{\omega_D}{\omega_e}\right)^2 (1 - 3\cos^2\beta)^2 \\ & \times \left\{ -\frac{3\sqrt{2}}{2} + \left(\frac{\omega_e}{\omega_1'}\right)\sin\omega_e t + \frac{11\sqrt{2}}{3}\cos\omega_e t \right. \\ & + \left(\frac{\omega_e}{\omega_1'}\right)\left(\frac{0.9\pi\sqrt{2}}{4} - \frac{11}{6}\right) \\ & \left. \times \sin 2\omega_e t + \frac{11\sqrt{2}}{6}\cos 2\omega_e t \right\} \\ & \times \cos\omega t + \sum_{n=1,2} \sum_{\lambda=\pm 1} A_{n,\lambda}^{(s)}(\beta)[\cos(n\omega_e + \lambda\Delta)t \\ & - \cos\omega_e t]\sin\omega t + \sum_{n=1,2} \sum_{\lambda=\pm 1} B_{n,\lambda}^{(s)}(\beta) \\ & \times [(-1)^n \sin(n\omega_e + \lambda\Delta)t - \sin\omega_e t]\sin\omega t \\ & + \sum_{\lambda=\pm 1} a_\lambda^{(s)}(\beta)\left[\left(\frac{3\omega_e + \lambda\Delta}{\omega_e}\right)\sin\omega_e t \right. \\ & \left. - \sin(\omega_e + \lambda\Delta)t + 2\sin(2\omega_e + \lambda\Delta)t\right] \\ & \times \sin\omega t + \sum_{n=1,2} \sum_{\lambda=\pm 1} A_{n,\lambda}^{(c)}(\beta)[\cos(n\omega_e + \lambda\Delta)t \\ & - \cos\omega_e t]\cos\omega t + \sum_{n=1,2} \sum_{\lambda=\pm 1} B_{n,\lambda}^{(c)}(\beta) \\ & \times [(-1)^n \sin(n\omega_e + \lambda\Delta)t - \sin\omega_e t]\cos\omega t \\ & + \sum_{n=1,2} \sum_{\lambda=\pm 1} D_{n,\lambda}^{(c)}(\beta)[1 - \cos(n\omega_e + \lambda\Delta)t]\cos\omega t \\ & + \sum_{n=1,2} \sum_{\lambda=\pm 1} F_{n,\lambda}^{(c)}(\beta)\sin(n\omega_e + \lambda\Delta)t\cos\omega t \\ & + \sum_{\lambda=\pm 1} a_\lambda^{(c)}(\beta)\left[\frac{\lambda\Delta}{\omega_e} - \left(\frac{3\omega_e + \lambda\Delta}{\omega_e}\right)\right. \\ & \times \cos\omega_e t - \cos(\omega_e + \lambda\Delta)t \\ & \left. - 2\cos(2\omega_e + \lambda\Delta)t\right]\cos\omega t. \end{aligned} \qquad [28]$$

$M_0 = \gamma_p \hbar \mathrm{Tr}\{\sigma_0(0) I_Z\}$; the symbol $\hbar\Delta$ is the A–E tunneling splitting; $\omega_e = \omega_1\sqrt{(\frac{3}{2})}$; β denotes the angle between the external magnetic field $\vec{H}_0$ and the symmetry axis of the methyl group; and the coefficients A to F and a are given in the Appendix. Due to the vanishing of the secular part of the dipolar interaction H_D^{00} [18, 20a] in the magic-angle frame, the frequencies corresponding to the transitions among the eigenstates of H_0 induced by the nonsecular terms [19] ($[H_0, V] \neq 0$) are not shifted by the dipolar interaction (as can be seen from [28]). The intensities of these transitions, on the other hand, do depend on the strength of the nonsecular part of the dipolar interaction in the tilted rotating frame [19, 20b, 20c] as shown in the Appendix.

DISCUSSION OF THE RESULTS

To represent the results in a graphical form, it is convenient to define the Fourier transform of $M_x(t)$ as

$$m_x(\tilde{\omega}, \cos\beta) = \frac{1}{\sqrt{2\pi}} \int_{-\infty}^{\infty} dt M_x(t) e^{i\tilde{\omega}t}, \qquad [29]$$

and the corresponding expression for a polycrystalline sample is

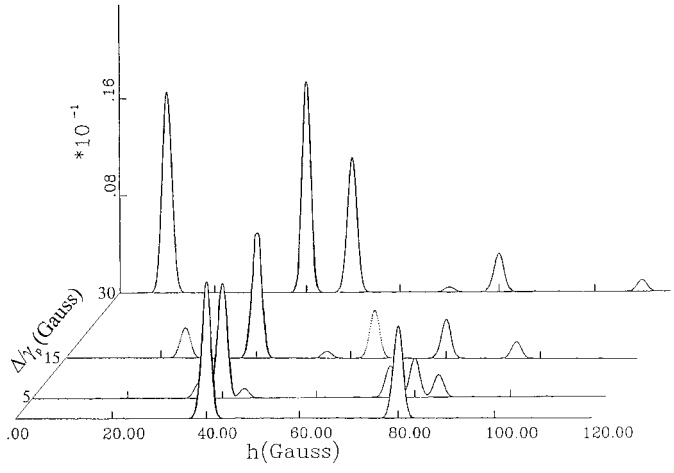

FIG. 1. The absolute value of the real part of the Fourier transform of the expression [28] corresponding to the magic-angle case. Here $H_e = 40$ G; the strength of the θ_M-pulse $H_1' = 50$ G; $\omega_D/\gamma_p = 5$ G, and the tunneling splitting Δ/γ_p is 0, 5, 15, and 30 G; the broadening parameter σ is 1 G. The curves are plotted as functions of Ω/γ_p (the imaginary part of the Fourier transform is qualitatively similar).

$$\langle m_x(\tilde{\omega})\rangle = \frac{1}{2}\int_{-1}^{1} d\,\cos\beta m_x(\tilde{\omega},\cos\beta). \qquad [30]$$

Using [28], [29], and [30] and the results given in the Appendix, it is not difficult to obtain the explicit results for $\langle m_x(\Omega)\rangle$ ($\Omega \equiv \tilde{\omega} - \omega$). Broadening the result with a Gaussian function according to

$$\langle m_x(\Omega;\,\sigma)\rangle = \int_{-\infty}^{\infty} du\langle m_x(u)\rangle e^{-(\Omega-u)^2/2\sigma^2}/\sqrt{2\pi\sigma^2}, \qquad [31]$$

we obtain the spectra shown in Fig. 1, representing the absolute value of the real part of the Fourier transform of [28]. (The imaginary component is not shown since in the magic-angle case it is qualitatively the same as the real part of the Fourier transform.)

It is well known (*8*) that the Fourier transform of the Zeeman polarization in the rotating frame at exact resonance shows nonvanishing intensity only in the vicinity of $2H_1$ (we are interested only in the Fourier components peaked at H_1 and $2H_1$ and neglect the Fourier component at $\Omega = 0$, which, although always present, is distorted due to experimental limitations). This is due to the fact that at exact resonance $\theta = \pi/2$, $d_{0\pm1}(\pi/2) = 0$, and V, as defined by [19], contains only the $V^{\pm2}$ terms of the dipolar interaction. This result, together with the assumption that $\sigma(0)$ in the rotating frame has the canonical form $\sigma(0) \propto e^{-\beta_Z H_Z - \beta_L(H_R + H_D^{00}(\pi/2))}$ is sufficient to show that the Fourier transform of the magnetization in the rotating frame has a nonvanishing intensity only near multiples of $2H_1$ (apart, of course, from the tunneling sidebands). However, when the evolution of the Zeeman-rotational system during the 90 or $\theta°$ pulse is allowed for, then the Fourier transform acquires intensity at multiples of H_1 as well, with intensity proportional to $\beta_Z|H_Z|\cdot\hbar\omega_D/\hbar\omega_1'$. This structure disappears in the limit $H_1' \to \infty$ and is in fact barely visible when H_1' is $\geq$60 G.

The situation is somewhat different when the experiments are performed off-resonance at the magic angle $\theta_M = \cos^{-1}(1/\sqrt{3})$. In this case, as was already pointed out, $d_{00}(\theta_M) = 0$, and consequently $H_D^{00}(\theta_M) = 0$; however, $d_{0k}(\theta_M) \neq 0$ for $k \neq 0$, and the real part of the Fourier transform of the x-component of the magnetization as given by [28] will have nonvanishing intensity both at H_1 and $2H_1$, even in the limit of a very strong θ_M° pulse. The imaginary component of the Fourier transform, due to the evolution of the Zeeman-rotational system during the θ_M° pulse, vanishes in this limit.

It holds true that the real component of the Fourier transform does not depend significantly on the strength of the θ_M° pulse for the Δ-values used. Simulations for $H_e = \sqrt{(\frac{3}{2})}H_1 = 40$ G, $H_1' = 50$ G, $\sigma = 1$ G, and $\Delta/\gamma_p = 0$, 5, 15, and 30 G are shown in Fig. 1. The curves are plotted as a function of the off-field parameter $h \equiv \Omega/\gamma_p$, with intensity given in arbitrary units. Only the real part of the Fourier transform is shown since the imaginary component is, at least for the parameters chosen, quantitatively the same.

COMPARISON WITH EXPERIMENTS

As has already been pointed out, at exact resonance ($\theta = \pi/2$), the real component of the Fourier transform $\langle m_x(\Omega;\,\sigma)\rangle$ shows a nonvanishing intensity only in the neighborhood of $2H_1$. Specifically, at $\Delta = 0$ there is a single peak centered at $2H_1$ of width of 3.8 G at half intensity. As the tunneling splitting $\hbar\Delta$ increases, a double peak structure appears at relatively small values of Δ. The peak-to-peak separation of the resulting tunneling satellite is further shifted by the dipolar interaction away from the expected value of 2Δ, with the magnitude of the shift dependent on the ratio ω_D/Δ.

At magic angle $H_D^{00}(\theta_M) = 0$ and consequently the tunneling satellites are not shifted by the dipolar interaction. It turns out that the agreement between the calculated and measured spectra is much better at $\theta = \theta_M$ than at exact resonance. We can see that the spectrum of CH_3CD_2I, Fig. 2a (*9*), taken at 40 K and $\theta = \theta_M$, compares well with the calculated results at θ_M, $H_1' = 25$ G, $H_e = 20$ G, and $\Delta/\gamma_p = 4.4$ G. The same is true in the case of methylmalonic acid, Fig. 3, with $\Delta/\gamma_p = 17.6$ G. A comparison of the on-resonance spectrum with its magic-angle counterpart (Figs. 3a and 3b, respectively) illustrates the improved spectral resolution obtainable with tilted rotating frame spectroscopy.

To conclude we would like to emphasize that the magnetization as given by [27] or [28] is evaluated immediately after

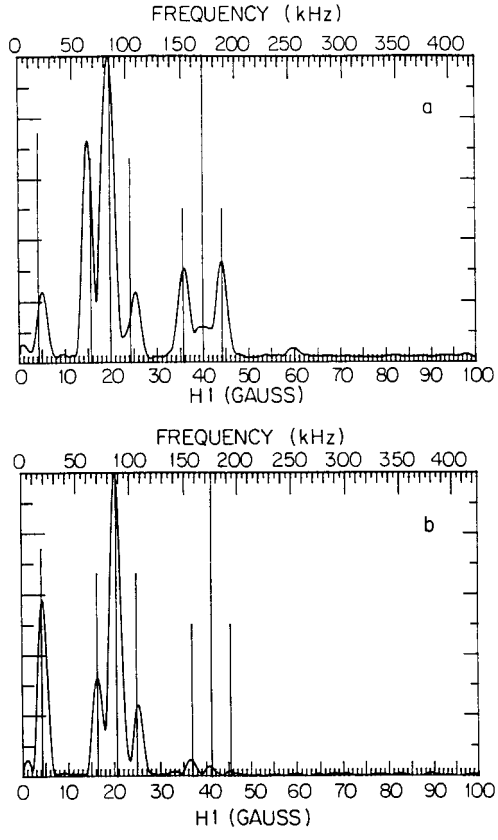

FIG. 2. The experimental spectrum of the proton magnetization evolution of CH_3CD_2I in the tilted rotating frame, at 40 K. (a) $H_e = 20$ G and $\theta = 65.9°$; (b) $H_e = 20$ G and $\theta = \theta_M$. Comparing this spectrum with that of Fig. 1 gives $\Delta/\gamma_p = 4.5 \pm 0.3$ G. Note the "nonmagnetic" peak at $0 + \Delta/\gamma_p \approx 4.5$ G. The $\Delta M = 1$ satellites are larger in the "half magic" ($\theta = 65.9°$) frame due to incomplete removal of the dipolar interaction. The solid reference lines shown indicate the expected values of the following resonances (left to right): $0 + \Delta/\gamma_p$; $\omega_e - \Delta/\gamma_p$; ω_e; $\omega_e + \Delta/\gamma_p$; $2\omega_e - \Delta/\gamma_p$; $2\omega_e$; $2\omega_e + \Delta/\gamma_p$. (Line heights are drawn to indicate spectral groupings (in order of decreasing height) corresponding to H_1 and $2H_1$, and the $\Delta M = 0$, 1, and 2 tunnelling transition satellites.)

the end of the field pulse H_1. However, the measurement of the FID is always delayed for a time τ ($\cong 10$ μs) after the end of the field pulse. For this reason we should also have taken into account the evolution of the magnetization in the laboratory frame under the action of $-\hbar\omega_0 I_Z + H_R + H_D^{00}$ (using the secular part of the dipolar interaction as defined in the laboratory frame). A calculation entirely analogous to the one described above shows that the real and imaginary components of the Fourier transform of $\langle I_x(t + \tau)\rangle$ become mixtures of the real and imaginary parts as defined on the basis of [27]. The corresponding weight factors are rapidly oscillating functions of the time delay τ. Consequently, when comparing the calculated spectra [28] with experimental results, this fact should be kept in mind. Moreover the τ-evolution causes the appearance of a line centered at the off-field value corresponding to the tunneling frequency, with intensity comparable to that of the lines centered around $2H_1$ (*10, 11*). These lines can be seen in the experimental results, Figs. 2 and 3.

CONCLUSIONS

In summary, we have presented a set of calculations for the time evolution of the proton Zeeman magnetization of an isolated tunneling methyl group in a tilted rotating frame and have found the resulting calculated spectra to be in good agreement with experimental results for CH_3CD_2I and methylmalonic acid. We have found, moreover, that spectral resolution and signal-to-noise are both considerably improved as the orientation angle approaches $\theta = \theta_M = \cos^{-1}(1/\sqrt{3})$, demonstrating that Fourier transform spectroscopy of the magnetization evolution in a tilted RF frame represents an excellent alternative to the analogous experiment performed at exact resonance.

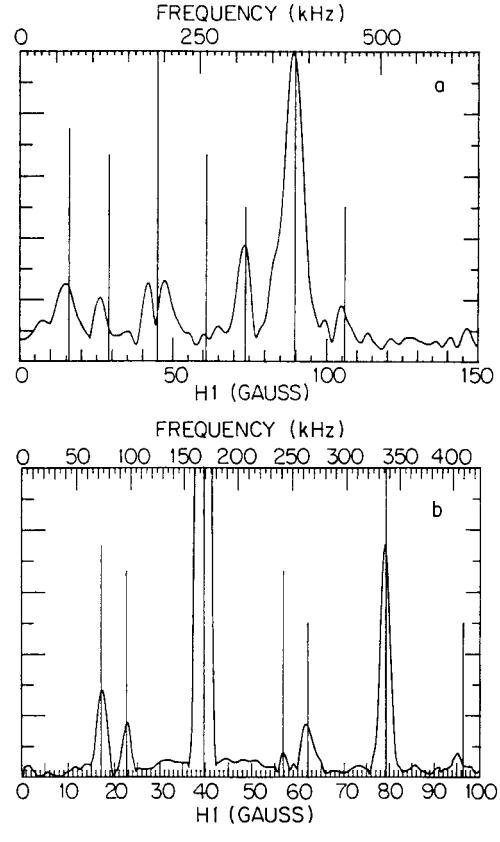

FIG. 3. The experimental spectrum of the proton magnetization evolution of methylmalonic acid at 30 K. (a) On-resonance rotating frame ($\theta = 90°$), real component with $\omega_1/\gamma_p \cong 45$ G. (b) Tilted rotating frame, with $\theta = \theta_M$ and $H_e = \omega_e/\gamma_p \cong 39.5$ G. A comparison of this spectrum with that of Fig. 1 gives $\Delta/\gamma_p = 17 \pm 0.5$ G. Note the "nonmagnetic" peak at $0 + \Delta/\gamma_p \approx 17.5$ G. The solid reference lines shown in (a) indicate the expected values of the following resonances (left to right): $0 + \Delta/\gamma_p$; $\omega_1 - \Delta/\gamma_p$; ω_1; $\omega_1 + \Delta/\gamma_p$; $2\omega_1 - \Delta/\gamma_p$; $2\omega_1$; $2\omega_1 + \Delta/\gamma_p$. The meaning of the reference lines in (b) and their height in both (a) and (b) are the same as that of Fig. 2.

APPENDIX

$$A^{(s)}_{1,\lambda}(\beta) = M_0 \frac{27}{128}\left(\frac{1}{3} + \cos\left(\frac{0.3\pi\Delta}{\omega_1'}\right)\right) \times (\sin^4\beta)\left(\frac{\omega_1'^{\,2}}{\Delta^2 - 4\omega_1'^{\,2}}\right)\frac{\omega_D^2}{\omega_1'(2\omega_e + \lambda\Delta)},$$

$$A^{(s)}_{2,\lambda}(\beta) = M_0 \frac{27\sqrt{2}}{64}\left(\frac{\sqrt{2}}{3} - \frac{\sin(0.3\pi\Delta/\omega_1')}{\Delta/\omega_1'}\right) \times (\sin^4\beta)\left(\frac{\omega_1'^{\,2}}{\Delta^2 - 4\omega_1'^{\,2}}\right)\frac{\omega_D^2}{\omega_1'(\omega_e + \lambda\Delta)},$$

$$B^{(s)}_{1,\lambda}(\beta) = M_0 \frac{27}{256}\left(\frac{\Delta\sqrt{2}}{3\omega_1'} - \sin\left(\frac{0.3\pi\Delta}{\omega_1'}\right)\right) \times (\sin^4\beta)\left(\frac{\omega_1'^{\,2}}{\Delta^2 - 4\omega_1'^{\,2}}\right)\frac{\omega_D^2}{\omega_1'(2\omega_e + \lambda\Delta)},$$

$$B^{(s)}_{2,\lambda}(\beta) = M_0 \frac{27\sqrt{2}}{128}\left(\frac{\Delta}{3\omega_1'} - \frac{1 - \cos(0.3\pi\Delta/\omega_1')}{\Delta/\omega_1'}\right) \times (\sin^4\beta)\left(\frac{\omega_1'^{\,2}}{\Delta^2 - 4\omega_1'^{\,2}}\right)\frac{\omega_D^2}{\omega_1'(\omega_e + \lambda\Delta)}$$

$$A^{(c)}_{1,\lambda}(\beta) = \frac{\sqrt{3}}{3} B^{(s)}_{1,\lambda}(\beta),\ A^{(c)}_{2,\lambda}(\beta) = -\frac{\sqrt{3}}{3} B^{(s)}_{2,\lambda}(\beta),$$

$$B^{(c)}_{1,\lambda}(\beta) = -\frac{\sqrt{3}}{3} A^{(s)}_{1,\lambda}(\beta),\ B^{(c)}_{2,\lambda}(\beta) = -\frac{\sqrt{3}}{3} A^{(s)}_{2,\lambda}(\beta),$$

$$a^{(s)}_{\lambda}(\beta) = -M_0 \frac{9\sqrt{2}}{128}(\sin^4\beta)\left(\frac{\omega_D^2}{(2\omega_e + \lambda\Delta)(\omega_e + \lambda\Delta)}\right),$$

$$a^{(c)}_{\lambda}(\beta) = \frac{\sqrt{3}}{3} a^{(s)}_{\lambda}(\beta),$$

$$D^{(c)}_{1,\lambda}(\beta) = -M_0 \frac{27}{128}\sqrt{\frac{2}{3}}\left[\frac{2}{3} + \frac{\omega_1'(\omega_e + \lambda\Delta)}{(\Delta^2 - 4\omega_1'^{\,2})}\left(\frac{2\lambda\Delta}{3\omega_1'} - \sqrt{2}\sin\left(\frac{0.3\pi\lambda\Delta}{\omega_1'}\right)\right)\right](\sin^4\beta)\frac{\omega_D^2}{(\omega_e + \lambda\Delta)^2}$$

$$D^{(c)}_{2,\lambda}(\beta) = -M_0 \frac{27}{128}\sqrt{\frac{2}{3}}\left\{\frac{4}{3} + \left(\frac{\omega_1'^{\,2}}{\Delta^2 - 4\omega_1'^{\,2}}\right) \times \left[\frac{4}{3}\frac{\lambda\Delta(2\omega_e + \lambda\Delta)}{\omega_1'^{\,2}} - \frac{4(2\omega_e + \lambda\Delta)}{\lambda\Delta} \times \left(1 - \cos\left(\frac{0.3\pi\Delta}{\omega_1'}\right)\right)\right]\right\} \times (\sin^4\beta)\left(\frac{\omega_D^2}{(2\omega_e + \lambda\Delta)^2}\right)$$

$$F^{(c)}_{1,\lambda}(\beta) = -M_0 \frac{27}{128}\sqrt{\frac{2}{3}}\frac{\omega_1'(\omega_e + \lambda\Delta)}{(\Delta^2 - 4\omega_1'^{\,2})}\left(\frac{\sqrt{2}}{3} + \sqrt{2}\cos\left(\frac{0.3\pi\Delta}{\omega_1'}\right)\right)(\sin^4\beta)\frac{\omega_D^2}{(\omega_e + \lambda\Delta)^2},$$

$$F^{(c)}_{2,\lambda}(\beta) = -M_0 \frac{27}{128}\sqrt{\frac{2}{3}}\left(\frac{\omega_1'^{\,2}}{\Delta^2 - 4\omega_1'^{\,2}}\right) \times \left[\frac{4(2\omega_e + \lambda\Delta)}{\Delta}\sin\left(\frac{0.3\pi\Delta}{\omega_1'}\right) - \frac{4\sqrt{2}}{3} \times \left(\frac{2\omega_e + \lambda\Delta}{\omega_1'}\right)\right](\sin^4\beta)\frac{\omega_D^2}{(2\omega_e + \lambda\Delta)^2}.$$

REFERENCES

1. W. Press, "Single Particle Rotations in Molecular Crystals," Springer Tracts in Modern Physics, Springer-Verlag, Berlin (1981).
2. J. Peternelj and I. Jencic, *J. Phys. A Math. Gen.* **22,** 1941 (1989).
3. J. Peternelj and T. Kranjc, *Phys. B* **240,** 343 (1997).
4. J. Peternelj, I. Jencic, B. Cvikl, and M. M. Pintar, *Phys. Rev. B* **35,** 25 (1987).
5. P. S. Hubbard, *Rev. Mod. Phys.* **33,** 249 (1961).
6. C. P. Slichter, "Principles of Magnetic Resonance—Third Enlarged and Updated Edition," Springer-Verlag, Berlin (1990).
7. A. Damyanovich, J. Peternelj, and M. M. Pintar, *J. Magn. Reson.* **140,** 9 (1999).
8. D. W. Nicoll and M. M. Pintar, *Phys. Rev. B* **23,** 1064 (1981).
9. A. Damyanovich, J. Peternelj, and M. M. Pintar, *Phys. B* **202,** 273 (1994).
10. M. J. Barlow, S. Clough, P. A. Debenham, and A. J. Horsewill, *J. Phys. C* **4,** 4165 (1992).
11. J. Peternelj, A. Damyanovich, and M. M. Pintar, *Phys. Rev. Lett.* **82,** 2587 (1999).